

BALKANTRIB'05
5th INTERNATIONAL CONFERENCE ON TRIBOLOGY
JUNE.15-18. 2005
Kragujevac, Serbia and Montenegro

**LOAD CARRIAGE PERFORMANCE OF JOURNAL
BEARINGS CONSIDERING EFFECTS OF TRANSVERSE
AND LONGITUDINAL PROFILE**

Cem SİNANOĞLU, Fazıl CANBULUT, Fehmi NAİR, Eyüp Sabri TOPAL

Mechanical Engineering Department, Engineering Faculty,

Erciyes University, 38039 Kayseri-TURKEY

To inspect the performance characteristics of journal bearing systems, the presence of transverse and longitudinal roughness on journal-bearing surfaces are studied using a proposed neural networks in this article.

The proposed network is capable of predict the performance characteristics of the experimental system. It can be outlined from the results for both approaches, neural network could be modelled journal bearing systems in practical applications.

Key Words: *Surface texture, journal bearing and neural nets*

1. INTRODUCTION

Journal bearings form great majority of hydrodynamic bearings used in industry. The field of application for journal bearings is immense. In journal bearings, the load supporting hydrodynamic pressure is very important [1]. During hydrodynamic lubrication, a pressure field forms in oil layer depending on the kinematics of the surface and geometrical conditions. It is essential the oil film to be convergent in order to form a pressure distribution to carry on applied load.

The hydrodynamic lubrication theory of rough surfaces has been studied with considerable interest in recent years. This is mainly because, all bearing surfaces, are rough to some extent and generally the roughness asperity height is of the same order as the mean separation between the lubricated contacts. Under such conditions surface roughness of the bearings considerably affects its performance.

The influence of the roughness parameter and the roughness patterns (longitudinal, transverse and isotropic) on the steady state and dynamic characteristics of hydrodynamic journal bearings with rough surfaces has been studied by Turaga et al. [2]. It was seen that the transverse roughness tended to increase significantly load carrying capacity and stability with roughness values whereas in the case of other roughness patterns the effect was seen to be very small.

Zhang and Qui [3] investigated the effects of two-sided purely longitudinal, transverse and isotropic surface roughness on the hydrodynamic lubrication of dynamically loaded journal bearings. They used Christensen's stochastic models for hydrodynamic lubrication of rough surfaces and considered the running in effect on roughness height distributions.

A theoretical study of the influence of circumferential, axial and combined surface waviness, present in journal bearing liners, on the performance of the bearings was presented by Rasheed [4]. It was shown that the presence of circumferential waviness increases the load carrying capacity and decreases the friction variable. But the axial waviness was shown to always have an adverse effect on the load

capacity and friction variable. The combined waviness was shown to enhance the load capacity and friction characteristics.

In this study, the effects of shaft surface texture on the performance of bearing pressure and consequently on the load were investigated experimentally and theoretically. In order to determine the effects of surface texture on the capacity of load carriage, the experiments were conducted at 18 °C for steel shaft systems with different surface textures (Smooth, Longitudinal and Transverse). The rotational speed was fixed at 1000, 1500 and 2500 rpm. The experimental data is employed as training and testing data for a proposed artificial neural network.

2. EXPERIMENTAL SYSTEM

The journal bearing test rig is described in Figure 1. In this section essentially consists of a clear perspex journal bearing assembled freely on a steel journal shaft (A). The large diameter journal shaft is directly fixed onto a motor shaft (B). The standard equipment control unit controls the speed of the motor shaft. With this system a speed range of between 500-3000 rev/min can be obtained.

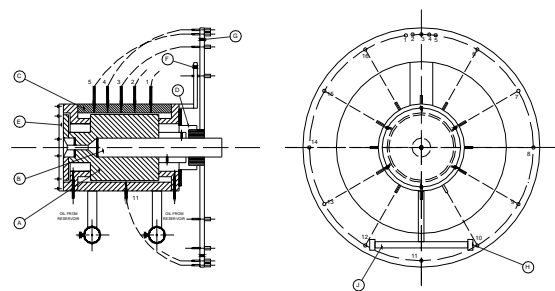
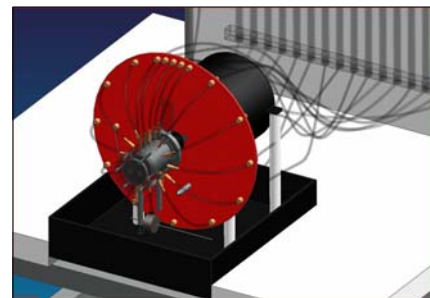


Figure 1: Journal bearing test rig

The journal bearing (C) has twelve equispaced pressure tappings around its circumference and four additional pressure tappings along its width. The latter four tappings fixed on the topside of the bearing are sealed by the flexible rubber diaphragm (D) and the other by the clear perspex disc and sealing ring (E). A cursor (F) fixed to the journal bearing at its rear end moves against a single engraved line on a fixed frame (G). When the bearing is in its normal position, the cursor and frame mark because in line. Small weight (H) added to the two-rod (J) during the test to maintain the bearing in its normal position when taking readings. The weights are freely adjustable along the rods. Oil film pressures are monitored in 16 tubes of 180-cm length. Journal bearing parameters are given in Table 1.

Table 1. The parameters of the bearing system

Parameters	Value
Diameter of the Journal ($2r$)	54.80 mm
Diameter of the bearing ($2R$)	55 mm
Effective bearing width	70 mm
Overall bearing width	80 mm
Dry weight of bearing width attachment	650 g
Weight of each movable load	100 g
Volume of oil carried in bearing	65.5 cm ³
Kinematics viscosity used lubricant (Mobil SHC-629-100 °C)	18.3 cSt

Various rotational speeds (1000, 2000 and 3000 rpm) were employed. Mobil SHC-629 synthetic oil was used as lubricant.

In the experimental study, motor rotation direction was selected to be in the clockwise and then, the motor was switched on and the speed was gradually increased to 1500 rpm. After that the speed was reduced from 1500 to 1000 rpm and the bearing was allowed to settle down in ten minutes. The required loads were added on to the shaft at the bottom, and then an angular displacement was formed in the bearing. When the manometer levels were settled down, the pressure reading on 16 manometers were taken. Initially, oil tank was fixed 735 mm levels (oil supply head $P_s = 735$ mm).

The pressure, which is constant due to on axial direction, indicated by 1, 2,...5 tubes are placed along the bearing axis. At the experimental work (Figure 1), the masses (H) on the (J) shaft can be placed on different positions. The

pressure values on the journal bearing were measured from 3, 6, 7, 8, 9, 10, 11, 12, 13, 14, 15 and 16 th tubes. The tube number also indicates the angles, i.e. 3 (0 and 360°), 6 (30°), 7 (60°), 8 (90°), 9 (120°), 10 (150°), 11 (180°), 12 (210°), 13 (240°), 14 (270°), 15 (300°) and 16 (330°). Pressure values from the tubes 3 (0 and 360°), 6 (30°), 7 (60°), 8 (90°), 9 (120°), 10 (150°), 12 (210°), 13 (240°), 14 (270°), 15 (300°) and 16 (330°) are used to testing data for ANNs.

3. ARTIFICIAL NEURAL NETWORKS

Artificial NN are non-linear mapping systems with a structure loosely based on principles observed in biological nervous systems. In the most general terms, a NN consist of large number of simple processors linked by weighted connections. It has many inputs (in) and one output (out). The connections between neurons are realised in the synapses (Figure 2).

- inputs x_1, x_2, \dots, x_n
- weights, bound to the inputs w_1, w_2, \dots, w_n
- an input function (f), which calculates the aggregated net input
- signal U to the neuron (this is usually a summation function)
- an activation (signal) function, which calculates the activation
- level of the neuron: $O = g(U)$

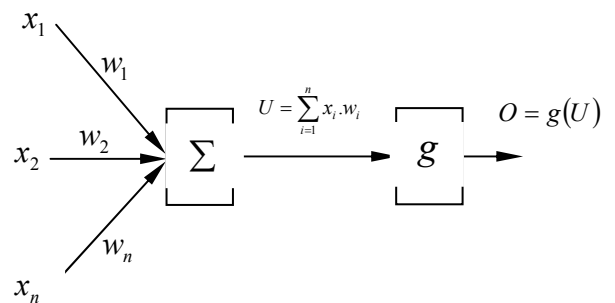


Figure 2: The artificial neuron model

A network is trained so that application of set inputs produces the desired (or at least consistent) set of outputs. Each such input (or output) set is referred to as a vector. Training is accomplished by sequentially applying input

vectors, while adjusting network weights according to a predetermined procedure. During training, the network weights gradually converge to values such that each input vector produces the desired output vector. The proposed neural network was trained with Quick propagation algorithm [5]. The activation (transfer) functions are possible for each hidden layer and the output layer. In this study, the tanh function [6] is used to hidden layers and output layers as an activation function. Linear function [7] is taken for input layer.

The structural and training parameters of the proposed network are given in Table 2. Moreover, average Rms errors for used training algorithm is shown in Table 3.

Table 2 The structural and training parameters

	η_i	μ	N	n_I	n_H	n_O	AF
Case 1-7	0.1	0	500000	1	10	3	tanh

Table 3 Average and maximum Rms error for training algorithm used

	Average RMS (%)
Case 1	0.0875
Case 2	0.1125
Case 3	0.0432
Case 4	0.0708
Case 5	0.0360
Case 6	0.0589
Case 7	0.0386
Case 8	0.0974

4. EXPERIMENTAL AND SIMULATION RESULTS

The bearing, which has a weight of 650 g, was run unloaded (only bearing weight) and loadings of 200 g each on the front and back loading rods, respectively (Figure 3).

The surface texture of the shaft with longitudinal profile is seen in Figure 3. Figure 4 (a) (Case 1) and (b) (Case 2) shows the variations of pressure differences versus the

angular position for Mobil SHC-629 lubricant and as the loads of 650 g (bearing load) and 650 g + 400 g were applied, respectively.

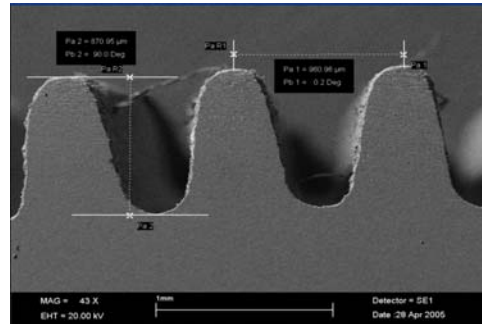


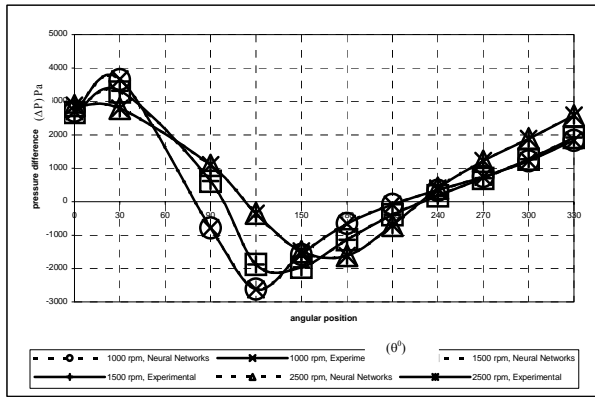
Figure 3: The surface texture of longitudinal shaft

In the Figure 4 (a), the measured pressure difference values on the 3, 6, 7, 12, 13, 14 and 15 pressure tubes were positive since the narrower oil wedge was between 0° and 90° , and between $240-330^{\circ}$. The other pressure differences values on the tubes 8, 9, 10, 11 thus between $120-210^{\circ}$ were negative. In these regions, since the narrowing oil wedge does not form, a negative pressure occurs.

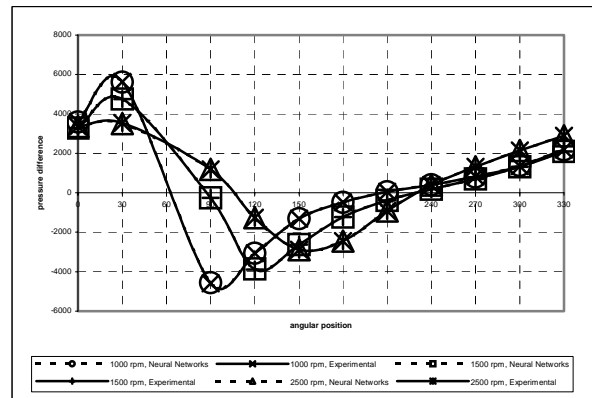
On the contrary, in the positive pressure regions the pressure increases up to 3670 pa for an angular velocity of 1000 rpm and 30° angular position. At this angular position, the minimum positive pressure difference is 2796 pa at 2500 rpm. Moreover, in this region corresponding to minimum oil film, the pressure differences are decreased with increasing revolutions.

Loss of pressure difference, ΔP , with increasing rpm is 874 pa. A loss of 23 % in pressure and hence in the load carrying capacity of the bearing was detected. In order to achieve a maximum pressure, the angular velocity of the shaft should be kept at 1000 rpm.

In the Figure 4 (b), the maximum pressure difference was fixed at 30° angular position. Its value was fixed at 5637 pa. The minimum positive pressure difference at the angular position of 30° is 3539 pa at 2500 rpm. When rpm rises to 2500 from 1000, the loss in the pressure difference loss is 37 %. ΔP is also decreased with increasing revolutions. The pressure difference levels are increased with increasing bearing load.



(a)



(b)

Figure 4: The pressure-angular values variation for experimental and neural network approaches

consisted of one input neurone, ten hidden layer neurones, three output neurones with (tanh) non-linear activation function. Network has good performance to predict such systems with all kinds of working conditions.

The shaft surface texture with transverse profile is presented in Figure 5. Figure 6 (a) (Case 3) shows the results of experimental and neural network assuming the variation of pressures with the transverse surface profile, at various angular positions and velocities with 650 g bearing load.

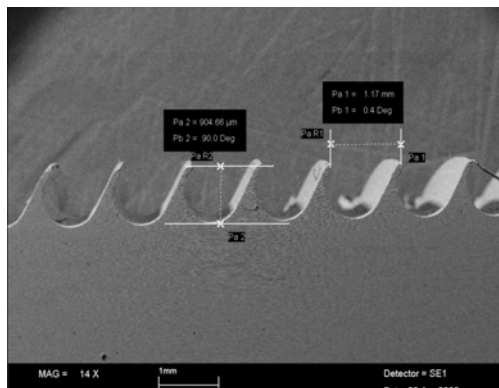


Figure 5: The surface texture of transverse shaft

Figure 6 (b) (Case 4) shows the pressure variations with the same shaft profile, at various speeds with 650 + 400 g load. The pressure differences values are 3889 pa (1000 rpm), 4195 pa (1500 rpm) and 3496 pa (2500 rpm) at 30°.

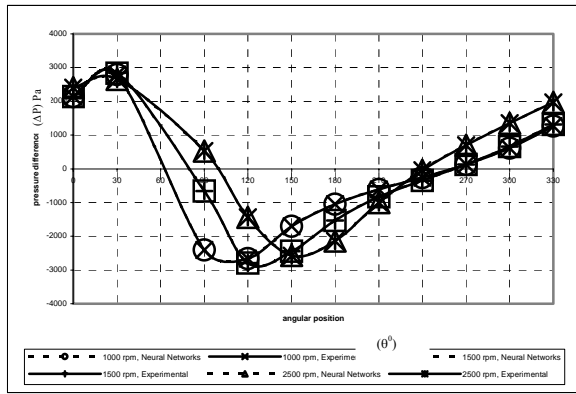
1000, the positive pressure difference is increased, but this pressure differences decreased between 1500-2500 rpm. The loss in the pressure difference loss is about 10 %. The designated neural predictor has also superior performance for modelling of the system.

Maximum positive difference of pressure occurs at the angular position $\theta \sim 30^\circ$, at 1500 rpm and it is 2796 pa (Figure 4 (a)).

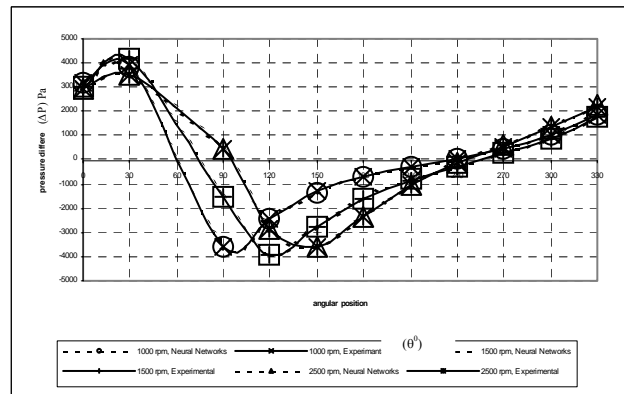
The minimum positive pressure difference at this position is 2665 pa at 2500 rpm. When rpm rises to 2500 from 1000, the loss in the pressure difference loss is about 4 %.

An additional shaft with smooth surface has also been used in order to test the effect of the surface texture of the shaft on the load-carrying capacity ($R_t = 6.0 \mu\text{m}$).

Figure 7 (a) (Case 5) and (b) (Case 6) shows the variation of pressure differences versus the angular position for Mobil SHC-629 lubricant and as the loads of 650 g and 650+ 400 g were applied, respectively. In the Figure 7 (a), the pressure difference values were positive at the angular positions of $0^\circ, 30^\circ, 60^\circ, 90^\circ, 270^\circ, 300^\circ$ and 330° corresponding to narrowing oil wedge region. The other pressures zones are negative. The maximum pressure difference is the velocity of 1000 rpm and 30° position (3190 pa). Minimum difference of pressure was found to be 2578 pa at this angular position and at 2500 rpm.



(a)



(b)

Figure 6: The pressure-angular values variation for experimental and neural network approaches

The loss of pressure difference was calculated to be 19 %. Figure 7 (a) also shows the results of neural network approach. As can be seen from this figure, the neural predictor has a high performance in designing an exact model of the lubricant system. Moreover, the difference of pressure is decreased with increasing number of revolution.

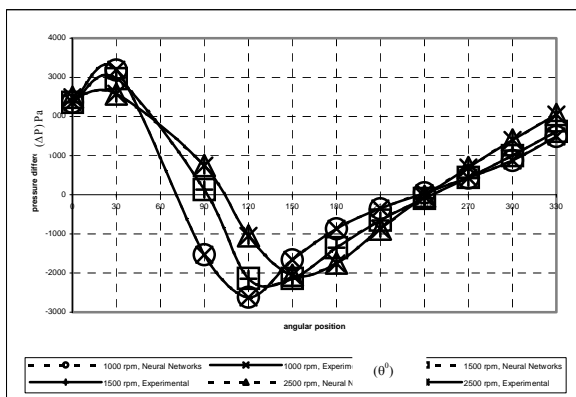
Because of the increasing bearing load, the pressure difference values in the Figure 7 (b) are higher than those in Figure 7 (a). In this figure, the pressure differences are also decreased with increasing speed. The minimum oil film occurs at 30° angular position. The maximum and minimum oil film pressures differences at this location are 4151 pa (1000 rpm) and 3583 pa (2500 rpm). The loss of pressure difference was calculated to be 13 %.

Figure 8 (Case 7) shows the pressure variations in different angular positions with a shaft having transverse, longitudinal profiles and smooth surface, 650 g bearing load at 1000 rpm using an experimental and neural network approach

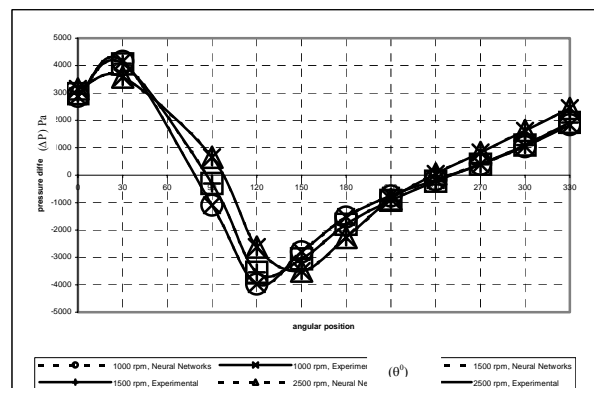
As is seen in Figure 8, maximum oil pressure occurs at an angular position of 30° . Since the static pressure is 5880 pa, the maximum pressure developing in the oil film when longitudinal, transverse and smooth surface shafts are run at 1000 rpm are 9550, 8676 and 9070 pa, respectively.

As we can see from the results, shaft with transverse profile bears the bearing load of 650 g with an oil pressure of a lower pressure level. Therefore, this shaft puts up a more favourable performance at lower rpm's. Furthermore, the loss of pressure on shaft with transverse profile is less when compared with the other shafts (4 %).

The pressure variations in different angular positions with a shaft having transverse, longitudinal profiles and smooth surface, 650 + 400 g load bearing at 1000 rpm using an experimental and neural network approach is shown in Figure 9 (Case 8).



(a)



(b)

Figure 7: The pressure-angular values variation for experimental and neural network approaches

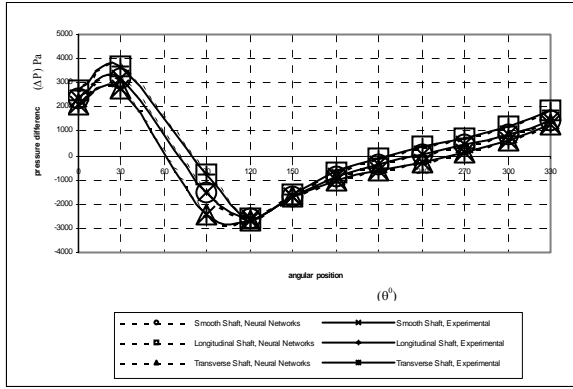


Figure 8: Pressure variations for different shafts for 1000 rpm and 650 g bearing load

As is seen in Figure 9, the maximum positive pressure difference occurs at 30° . These values are 5637 pa for shaft with longitudinal profile, 4151 pa for shaft with smooth surface and 3889 pa for shaft with transverse profile. Understandably, shaft with transverse profile displays a favourable performance as far as load carriage capacity is concerned.

The error convergence graphs of the case 6 and 7 are depicted in Figures 10 (a) and (b) during the training of the network.

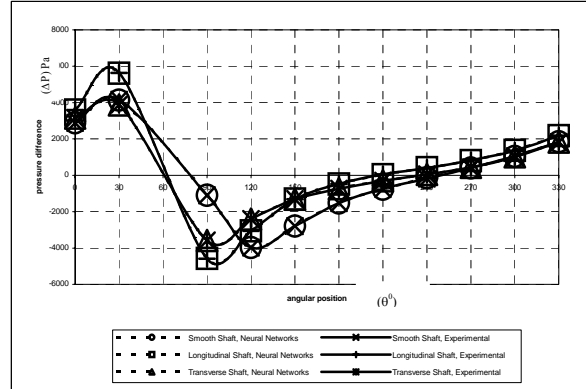
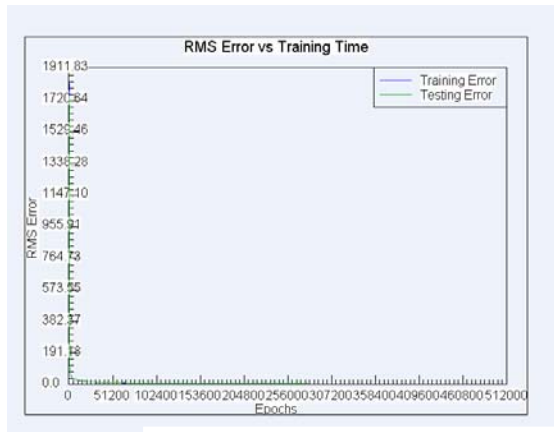
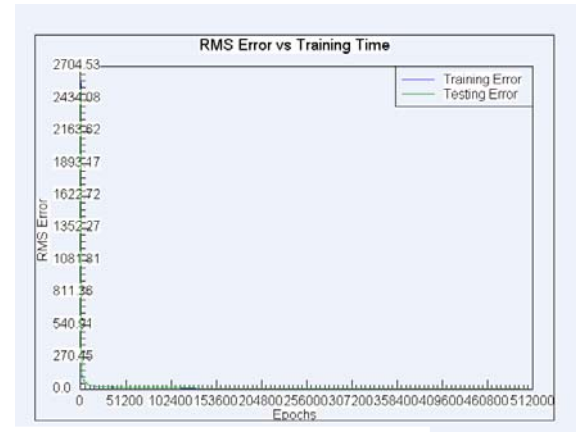


Figure 9: Pressure variations for different shafts for 1000 rpm and 650+400 g bearing load

The shaft with transverse profile carries the total bearing load of 1050 g with an oil pressure of a lower pressure level. Thus, greater loads can be borne at greater pressures when this shaft is used. As can be seen in the figure, the neural network results exactly follow the experimental results.



(a)



(b)

Figure 10: The error convergence graphs for case 6 and 7

5. CONCLUSIONS

In this paper, a neural network predictor has been employed to analyze of the effects of shaft surface profile in hydrodynamic lubrication of journal bearing. From the experimental and simulation results, neural network exactly follows the experimental results. Because of that, this kind of neural network predictors can be applied on journal bearing systems in real applications.

6. REFERENCES

- [1] Kurban, A.O. and Sinanoğlu, C. (2000), "Experimental investigation of elasto-hydrodynamic lubrication, pressure development and capability of bearing load at different ambient temperatures", Journal of The Balkan Tribological Association, Vol 6 No 1, pp. 19-26.

[2] Turaga, R., Sekhar, A.S. and Majumdar, B.C. (1999), "The effects of roughness parameter on the performance of hydrodynamic journal bearings with rough surfaces", *Tribology International*, Vol 32, pp. 231-236.

[3] Zhang, C. and Qiu, Z. (1998), "Effects of surface texture on hydrodynamic lubrication of dynamically loaded journal bearings", *STLE Tribology Transaction*, Vol. 41, pp. 43-48.

[4] Rasheed, H.E. (1998), "Effect of surface waviness on the hydrodynamic lubrication of a plain cylindrical sliding element bearing", *Wear*, Vol 223, pp. 1-6.

[5] Sinanoğlu, C., Kurban, A.O., Yıldırım, Ş. (2004), Analysis of Pressure Variations on Journal Bearing System Using Artificial Neural Network, *Industrial Lubrication and Tribology*, Vol. 56 No. 2, pp. 74-87.

[6] Bharath, R., Drosen, J., *Neural Network Computing*, Windcrest /Mc. Graw-Hill, 1994.

[7] Canbulut, F., Yıldırım, Ş. and Sinanoğlu, C. (2004), Design of An Artificial Neural Network for Analysis of Frictional Power Loss of Hydrostatic Slipper Bearings, *STLE Tribology Letters*, Vol. 17 No. 4, pp. 997-899.